

Geometry of Quantum Logic Gates

M. W. AlMasri^{1,*}

¹Wilczek Quantum Center, School of Physics and Astronomy,
Shanghai Jiaotong University, Minhang, Shanghai, China

In this work, we investigate the geometry of quantum logic gates within the holomorphic representation of quantum mechanics. We begin by embedding the physical qubit subspace into the space of holomorphic functions that are homogeneous of degree one in each Schwinger boson pair (z_{a_j}, z_{b_j}) . Within this framework, we derive explicit closed-form differential operator representations for a universal set of quantum gates—including the Pauli operators, Hadamard, CNOT, CZ, and SWAP—and demonstrate that they preserve the physical subspace exactly. Restricting to unit-magnitude variables ($|z| = 1$) reveals a toroidal space \mathbb{T}^{2N} , on which quantum gates act as canonical transformations: Pauli operators generate Hamiltonian flows, the Hadamard gate induces a nonlinear automorphism, and entangling gates produce correlated diffeomorphisms that couple distinct toroidal factors. Beyond the torus, the full Segal–Bargmann space carries a natural Kähler geometry that governs amplitude dynamics. Entanglement is geometrically characterized via the Segre embedding into complex projective space, while topological protection arises from the $U(1)^N$ fiber bundle structure associated with the Jordan–Schwinger constraint.

I. INTRODUCTION

The representation of quantum information in continuous phase space has long provided profound insights into the structure of quantum theory, from the Wigner–Weyl correspondence to modern formulations of quantum optics and quantum computation [1–4]. In [5], the authors represented both the states and the evolution of a quantum computer in phase space using the discrete Wigner function. This framework allows us to analyze quantum algorithms—such as the Fourier transform and Grover’s search—and to examine the conditions under which quantum evolution corresponds directly to classical dynamics in phase space. The Bargmann representation provides a holomorphic (complex-analytic) realization of quantum states in which wavefunctions are entire functions of a complex variable $z \in \mathbb{C}$, related to the phase-space coordinates via $z = \frac{q+ip}{\sqrt{2}}$ (in dimensionless units). In this representation, the standard phase space of classical mechanics—spanned by position q and momentum p —is identified with the complex plane, and quantum states correspond to square-integrable holomorphic functions with respect to the Gaussian measure $e^{-|z|^2} d^2z$. Coherent states map to simple monomials or exponentials, and operators act as differential operators, making the Segal–Bargmann space particularly well-suited for studying bosonic systems, semiclassical limits, and analytic properties of quantum dynamics. Thus, the Bargmann representation offers a powerful bridge between Hilbert space quantum mechanics and complex phase space geometry [6–12].

In this work, we construct an explicit and self-contained holomorphic representation of quantum logic gates by unifying these three transformations. We show that any N -qubit gate can be expressed as a differential

operator acting on Segal–Bargmann space functions that are homogeneous of degree one in each Schwinger boson pair (z_{a_j}, z_{b_j}) . This representation preserves the physical subspace exactly and provides a direct link between algebraic gate operations and geometric flows on phase space.

Our key contributions are threefold: (i) We derive closed-form differential operator expressions for fundamental single- and multi-qubit gates—including Pauli operators, Hadamard, SWAP, CNOT, and CZ—in terms of holomorphic variables. (ii) We analyze the induced dynamics on the toroidal space \mathbb{T}^{2N} obtained by restricting to unit-magnitude variables ($|z| = 1$), revealing that quantum gates act as canonical transformations with distinct geometric signatures (e.g., Hamiltonian flows for Pauli gates, nonlinear automorphisms for Hadamard). (iii) We uncover deeper geometric structures beyond the torus: the full Segal–Bargmann space carries a Kähler geometry governing amplitude dynamics; entanglement is characterized via the Segre embedding; and topological protection emerges from the $U(1)^N$ fiber bundle structure associated with the Jordan–Schwinger constraint. The remainder of this paper is structured as follows. In Sec. II, we present the foundational mapping from fermionic systems to holomorphic representation. We derive the homogeneity constraint that characterizes physical qubit states and show how computational basis states are encoded in holomorphic variables.

Section III presents the core result: explicit differential operator representations of universal quantum logic gates in the Segal–Bargmann space. We provide closed-form expressions for single-qubit gates (Pauli operators, Hadamard) and multi-qubit gates (SWAP, CNOT, CZ), demonstrating that all preserve the physical subspace.

In Sec. IV, we restrict to unit-magnitude variables ($|z| = 1$) to reveal the toroidal space \mathbb{T}^{2N} , where quantum gates act as canonical transformations. We analyze Pauli gates as Hamiltonian flows, Hadamard as a nonlinear automorphism, and entangling gates as diffeomor-

* mwalmasri2003@gmail.com

phisms that correlate distinct toroidal factors.

Section V extends the analysis beyond the torus to uncover deeper geometric structures: the Kähler geometry governing amplitude dynamics, the Segre embedding for entanglement characterization, the fiber bundle structure underlying topological protection, and the path integral formulation for semiclassical simulation.

Finally, Sec. VI summarizes our findings and discusses implications for quantum simulation, error analysis, and geometric quantum computing.

II. QUBITS IN HOLOMORPHIC REPRESENTATION

Consider a system of N fermionic modes with annihilation and creation operators c_j, c_j^\dagger satisfying the canonical anti-commutation relations:

$$\{c_i, c_j^\dagger\} = \delta_{ij}, \quad (1)$$

$$\{c_i, c_j\} = \{c_i^\dagger, c_j^\dagger\} = 0. \quad (2)$$

The Jordan–Wigner transformation maps these to spin- $\frac{1}{2}$ operators (Pauli matrices) on N qubits:

$$c_j = \left(\bigotimes_{k=1}^{j-1} \sigma_k^x \right) \otimes \sigma_j^-, \quad (3)$$

$$c_j^\dagger = \left(\bigotimes_{k=1}^{j-1} \sigma_k^x \right) \otimes \sigma_j^+, \quad (4)$$

where $\sigma_j^\pm = (\sigma_j^x \pm i\sigma_j^y)/2$, and $\sigma_j^x, \sigma_j^y, \sigma_j^z$ are Pauli matrices acting on qubit j . This mapping preserves the fermionic algebra through non-local string operators. Consequently, the fermionic Fock space \mathcal{F} is isomorphic to the N -qubit Hilbert space

$$\mathcal{H}_{\text{qubit}} = (\mathbb{C}^2)^{\otimes N}. \quad (5)$$

Each qubit (spin- $\frac{1}{2}$) is encoded into two bosonic modes a_j, b_j via the Schwinger boson representation:

$$\sigma_j^+ = a_j^\dagger b_j, \quad (6)$$

$$\sigma_j^- = b_j^\dagger a_j, \quad (7)$$

$$\sigma_j^z = a_j^\dagger a_j - b_j^\dagger b_j. \quad (8)$$

Physical states for qubit j are restricted to the subspace of total occupation number one:

$$\hat{n}_j^{\text{tot}} = a_j^\dagger a_j + b_j^\dagger b_j = 1. \quad (9)$$

Thus, the full N -qubit space $\mathcal{H}_{\text{qubit}}$ is isomorphic to the physical subspace $\mathcal{H}_{\text{boson}}^{\text{phys}} \subset \mathcal{F}_{\text{boson}}$ of the bosonic Fock space $\mathcal{F}_{\text{boson}}$ for $2N$ modes, characterized by

$$\hat{n}_j^{\text{tot}} |\psi\rangle = |\psi\rangle \quad \forall j = 1, \dots, N. \quad (10)$$

The bosonic Fock space $\mathcal{F}_{\text{boson}}$ is mapped to the Segal–Bargmann space \mathcal{H}_{SB} , consisting of holomorphic functions $f : \mathbb{C}^{2N} \rightarrow \mathbb{C}$ that are square-integrable with respect to the Gaussian measure

$$d\mu(\mathbf{z}) = e^{-\|\mathbf{z}\|^2} \prod_{j=1}^N \frac{d^2 z_{a_j} d^2 z_{b_j}}{\pi^2}, \quad (11)$$

where $\|\mathbf{z}\|^2 = \sum_{j=1}^N (|z_{a_j}|^2 + |z_{b_j}|^2)$.

The Bargmann map is defined by:

- Vacuum state: $|0\rangle \mapsto f_0(\mathbf{z}) = 1$,
- Creation operators: $a_j^\dagger \mapsto z_{a_j}, b_j^\dagger \mapsto z_{b_j}$,
- Annihilation operators: $a_j \mapsto \partial/\partial z_{a_j}, b_j \mapsto \partial/\partial z_{b_j}$.

The physical constraint $\hat{n}_j^{\text{tot}} = 1$ translates into the homogeneity condition

$$\left(z_{a_j} \frac{\partial}{\partial z_{a_j}} + z_{b_j} \frac{\partial}{\partial z_{b_j}} \right) f(\mathbf{z}) = f(\mathbf{z}) \quad \forall j. \quad (12)$$

Hence, physical states correspond to functions homogeneous of degree one in each pair (z_{a_j}, z_{b_j}) :

$$f(\mathbf{z}) = \sum_{\mathbf{s} \in \{0,1\}^N} c_{\mathbf{s}} \prod_{j=1}^N z_{a_j}^{1-s_j} z_{b_j}^{s_j}, \quad (13)$$

where $s_j = 0$ labels spin-up ($|\uparrow\rangle_j$) and $s_j = 1$ labels spin-down ($|\downarrow\rangle_j$).

III. HOLOMORPHIC REPRESENTATION OF QUANTUM LOGIC GATES

Following the construction outlined above, we now express fundamental quantum logic gates—namely the Pauli gates X, Y, Z , the Hadamard gate H , and the two-qubit SWAP gate—as differential operators acting on holomorphic functions $f(\mathbf{z}) \in \mathcal{B}$ that satisfy the homogeneity constraint

$$\left(z_{a_j} \partial_{z_{a_j}} + z_{b_j} \partial_{z_{b_j}} \right) f = f \quad \forall j. \quad (14)$$

In this representation, the logical basis states correspond to:

$$|0\rangle_j \equiv |\uparrow\rangle_j \mapsto z_{a_j}, \quad (15)$$

$$|1\rangle_j \equiv |\downarrow\rangle_j \mapsto z_{b_j}. \quad (16)$$

A. Single-Qubit Gates

Using the Schwinger boson mapping $\sigma_j^+ = a_j^\dagger b_j, \sigma_j^- = b_j^\dagger a_j, \sigma_j^z = a_j^\dagger a_j - b_j^\dagger b_j$, and applying the Bargmann correspondence, we obtain:

- **Pauli- X (bit-flip):**

$$X_j \mapsto z_{a_j} \partial_{z_{b_j}} + z_{b_j} \partial_{z_{a_j}}. \quad (17)$$

- **Pauli- Y (bit-phase flip):**

$$Y_j \mapsto -i \left(z_{a_j} \partial_{z_{b_j}} - z_{b_j} \partial_{z_{a_j}} \right). \quad (18)$$

- **Pauli- Z (phase flip):**

$$Z_j \mapsto z_{a_j} \partial_{z_{a_j}} - z_{b_j} \partial_{z_{b_j}}. \quad (19)$$

- **Hadamard gate:** The Hadamard gate acts as a linear transformation on the holomorphic coordinates:

$$(H_j f)(\dots, z_{a_j}, z_{b_j}, \dots) = f \left(\dots, \frac{z_{a_j} + z_{b_j}}{\sqrt{2}}, \frac{z_{a_j} - z_{b_j}}{\sqrt{2}}, \dots \right). \quad (20)$$

This is equivalent to the pullback under the orthogonal map $(z_{a_j}, z_{b_j}) \mapsto ((z_{a_j} + z_{b_j})/\sqrt{2}, (z_{a_j} - z_{b_j})/\sqrt{2})$.

- **Two-qubit SWAP gate:** The SWAP gate exchanges the holomorphic variables of two qubits:

$$\begin{aligned} (\text{SWAP}_{jk} f)(\dots, z_{a_j}, z_{b_j}, \dots, z_{a_k}, z_{b_k}, \dots) &= (21) \\ &= f(\dots, z_{a_k}, z_{b_k}, \dots, z_{a_j}, z_{b_j}, \dots). \end{aligned}$$

This permutation preserves the physical homogeneity condition and implements $\text{SWAP}_{jk} |s_j, s_k\rangle = |s_k, s_j\rangle$.

B. Multi-Qubit Gates

Multi-qubit gates are constructed by combining single-qubit operators across distinct mode pairs. Since each qubit j is encoded in its own bosonic pair (z_{a_j}, z_{b_j}) , gates acting on multiple qubits factorize naturally in the holomorphic representation.

- **Controlled-NOT (CNOT _{c,t}):** The CNOT gate flips the target qubit t if the control qubit c is in state $|1\rangle$. Using the projector $|1\rangle\langle 1|_c = \frac{1}{2}(1 - Z_c)$, we write:

$$\text{CNOT}_{c,t} = \frac{1 + Z_c}{2} + \frac{1 - Z_c}{2} X_t. \quad (22)$$

In Segal-Bargmann space \mathcal{H}_{SB} , this becomes:

$$\begin{aligned} \text{CNOT}_{c,t} &\mapsto \frac{1}{2} (1 + z_{a_c} \partial_{z_{a_c}} - z_{b_c} \partial_{z_{b_c}}) \\ &+ \frac{1}{2} (1 - z_{a_c} \partial_{z_{a_c}} + z_{b_c} \partial_{z_{b_c}}) (z_{a_t} \partial_{z_{b_t}} + z_{b_t} \partial_{z_{a_t}}). \end{aligned} \quad (23)$$

- **Controlled-Z (CZ _{c,t}):** The CZ gate applies a phase flip when both qubits are $|1\rangle$:

$$\text{CZ}_{c,t} = \frac{1}{2} (1 + Z_c + Z_t - Z_c Z_t). \quad (24)$$

Its Bargmann representation is:

$$\begin{aligned} \text{CZ}_{c,t} &\mapsto \frac{1}{2} \left[1 + (z_{a_c} \partial_{z_{a_c}} - z_{b_c} \partial_{z_{b_c}}) \right. \\ &+ (z_{a_t} \partial_{z_{a_t}} - z_{b_t} \partial_{z_{b_t}}) - (z_{a_c} \partial_{z_{a_c}} - z_{b_c} \partial_{z_{b_c}}) \\ &\left. \times (z_{a_t} \partial_{z_{a_t}} - z_{b_t} \partial_{z_{b_t}}) \right]. \end{aligned} \quad (25)$$

- **SWAP _{j,k} :** The SWAP gate admits the decomposition:

$$\text{SWAP}_{j,k} = \frac{1}{2} (1 + X_j X_k + Y_j Y_k + Z_j Z_k). \quad (26)$$

Substituting the differential forms yields:

$$\begin{aligned} \text{SWAP}_{j,k} &\mapsto \frac{1}{2} \left[1 \right. \\ &+ \left(z_{a_j} \partial_{z_{b_j}} + z_{b_j} \partial_{z_{a_j}} \right) \left(z_{a_k} \partial_{z_{b_k}} + z_{b_k} \partial_{z_{a_k}} \right) \\ &- \left(z_{a_j} \partial_{z_{b_j}} - z_{b_j} \partial_{z_{a_j}} \right) \left(z_{a_k} \partial_{z_{b_k}} - z_{b_k} \partial_{z_{a_k}} \right) \\ &\left. + \left(z_{a_j} \partial_{z_{a_j}} - z_{b_j} \partial_{z_{b_j}} \right) \left(z_{a_k} \partial_{z_{a_k}} - z_{b_k} \partial_{z_{b_k}} \right) \right]. \end{aligned} \quad (27)$$

- **General Controlled- U :** For any single-qubit unitary $U = u_{00} + u_{01}X + u_{10}Y + u_{11}Z$, the controlled- U gate is:

$$\Lambda_c(U_t) = \frac{1+Z_c}{2} + \frac{1-Z_c}{2} U_t, \quad (28)$$

with Bargmann representation obtained by substituting the differential forms of Z_c and U_t .

All multi-qubit gates preserve the local homogeneity condition $z_{a_j} \partial_{z_{a_j}} + z_{b_j} \partial_{z_{b_j}} = 1$ for every qubit j , ensuring they map physical states to physical states.

IV. PHASOR REPRESENTATION OF QUANTUM GATES

We now consider the restriction of the Bargmann representation to the unit circle, where each holomorphic variable is expressed in phasor form as

$$z_{a_j} = e^{i\phi_{a_j}}, \quad z_{b_j} = e^{i\phi_{b_j}}, \quad (29)$$

with $\phi_{a_j}, \phi_{b_j} \in [0, 2\pi)$. This corresponds to fixing the magnitude $|z| = 1$ while retaining the phase degree of freedom, which is sufficient to represent qubit states due to the homogeneity constraint $z_{a_j} \partial_{z_{a_j}} + z_{b_j} \partial_{z_{b_j}} = 1$.

Under this restriction, the physical state space becomes a torus \mathbb{T}^{2N} parameterized by the phase angles $\{\phi_{a_j}, \phi_{b_j}\}_{j=1}^N$. The basis states correspond to:

$$|0\rangle_j \equiv |\uparrow\rangle_j \mapsto e^{i\phi_{a_j}}, \quad (30)$$

$$|1\rangle_j \equiv |\downarrow\rangle_j \mapsto e^{i\phi_{b_j}}. \quad (31)$$

The differential operators transform according to the chain rule:

$$\frac{\partial}{\partial z_{a_j}} = \frac{\partial \phi_{a_j}}{\partial z_{a_j}} \frac{\partial}{\partial \phi_{a_j}} = -\frac{i}{z_{a_j}} \frac{\partial}{\partial \phi_{a_j}} = -ie^{-i\phi_{a_j}} \frac{\partial}{\partial \phi_{a_j}}, \quad (32)$$

and similarly for z_{b_j} . Substituting these into the gate representations yields:

A. Single-Qubit Gates in Phasor Form

- **Pauli- X (bit-flip):**

$$X_j \mapsto -i \left(e^{i(\phi_{a_j} - \phi_{b_j})} \frac{\partial}{\partial \phi_{b_j}} + e^{i(\phi_{b_j} - \phi_{a_j})} \frac{\partial}{\partial \phi_{a_j}} \right). \quad (33)$$

- **Pauli- Y (bit-phase flip):**

$$Y_j \mapsto - \left(e^{i(\phi_{a_j} - \phi_{b_j})} \frac{\partial}{\partial \phi_{b_j}} - e^{i(\phi_{b_j} - \phi_{a_j})} \frac{\partial}{\partial \phi_{a_j}} \right). \quad (34)$$

- **Pauli- Z (phase flip):**

$$Z_j \mapsto -i \left(\frac{\partial}{\partial \phi_{a_j}} - \frac{\partial}{\partial \phi_{b_j}} \right). \quad (35)$$

- **Hadamard gate:** The Hadamard transformation becomes a rotation in Segal–Bargmann space:

$$(H_j f)(\dots, \phi_{a_j}, \phi_{b_j}, \dots) = f \left(\dots, \arg \left(e^{i\phi_{a_j}} + e^{i\phi_{b_j}} \right), \arg \left(e^{i\phi_{a_j}} - e^{i\phi_{b_j}} \right), \dots \right), \quad (36)$$

where $\arg(z)$ denotes the principal argument of z . Equivalently, defining $\Delta\phi_j = \phi_{a_j} - \phi_{b_j}$, we have:

$$\phi'_{a_j} = \arg(1 + e^{i\Delta\phi_j}) = \frac{\phi_{a_j} + \phi_{b_j}}{2} + \frac{\pi}{2} - \arctan \left(\cot \frac{\Delta\phi_j}{2} \right), \quad (37)$$

$$\phi'_{b_j} = \arg(1 - e^{i\Delta\phi_j}) = \frac{\phi_{a_j} + \phi_{b_j}}{2} - \arctan \left(\tan \frac{\Delta\phi_j}{2} \right). \quad (38)$$

- **Two-qubit SWAP gate:** The SWAP operation exchanges phase angles between qubits:

$$(\text{SWAP}_{jk} f)(\dots, \phi_{a_j}, \phi_{b_j}, \dots, \phi_{a_k}, \phi_{b_k}, \dots) = f(\dots, \phi_{a_k}, \phi_{b_k}, \dots, \phi_{a_j}, \phi_{b_j}, \dots). \quad (39)$$

B. Geometric Interpretation on Toroidal Phase Space

The restriction to unit-magnitude holomorphic variables $z_{a_j} = e^{i\phi_{a_j}}$, $z_{b_j} = e^{i\phi_{b_j}}$ maps the physical subspace of Segal–Bargmann space \mathcal{H}_{SB} onto the $2N$ -torus $\mathbb{T}^{2N} = (S^1)^{2N}$, where each S^1 corresponds to a phase angle. Quantum states are then represented as functions $f(\phi)$ on this torus, and quantum gates act as canonical transformations that preserve the symplectic structure induced by the homogeneity constraint.

- **Pauli gates as Hamiltonian flows:** Each Pauli operator generates a Hamiltonian flow on the toroidal phase space \mathbb{T}^{2N} , governed by the symplectic form

induced by the homogeneity constraint. Specifically, the torus \mathbb{T}^{2N} carries a natural symplectic structure $\omega = \sum_{j=1}^N d\phi_{a_j} \wedge d\phi_{b_j}$, under which any real-valued function $H(\phi)$ defines a Hamiltonian vector field X_H via $\iota_{X_H} \omega = dH$. The Pauli operators correspond to linear Hamiltonians:

- For Z_j , the Hamiltonian is $H_{Z_j} = \phi_{a_j} - \phi_{b_j} = \Delta\phi_j$. The resulting flow is

$$\dot{\phi}_{a_j} = \frac{\partial H_{Z_j}}{\partial \phi_{b_j}} = -1, \quad \dot{\phi}_{b_j} = -\frac{\partial H_{Z_j}}{\partial \phi_{a_j}} = 1,$$

which integrates to straight-line trajectories:

$$\phi_{a_j}(t) = \phi_{a_j}(0) - t, \quad \phi_{b_j}(t) = \phi_{b_j}(0) + t.$$

Thus, Z_j generates uniform translation along the relative phase $\Delta\phi_j$, while the total phase $\Sigma\phi_j = \phi_{a_j} + \phi_{b_j}$ remains constant—corresponding to pure phase accumulation without population transfer.

- For X_j , the Hamiltonian is $H_{X_j} = \sin(\Delta\phi_j)$. The equations of motion are:

$$\dot{\phi}_{a_j} = \cos(\Delta\phi_j), \quad \dot{\phi}_{b_j} = -\cos(\Delta\phi_j),$$

yielding coupled oscillations in the (ϕ_{a_j}, ϕ_{b_j}) plane. In terms of sum and difference coordinates, this becomes:

$$\dot{\Sigma\phi}_j = 0, \quad \dot{\Delta\phi}_j = 2 \cos(\Delta\phi_j),$$

describing periodic exchange of amplitude between the two modes. The flow lines are level sets of $\Sigma\phi_j$, with fixed points at $\Delta\phi_j = \pm\pi/2$ (corresponding to eigenstates of X_j).

- Similarly, Y_j corresponds to the Hamiltonian $H_{Y_j} = -\cos(\Delta\phi_j)$, generating flows with fixed points at $\Delta\phi_j = 0, \pi$ (eigenstates of Y_j).

These flows are geodesics of the flat metric $g = \sum_j (d\phi_{a_j}^2 + d\phi_{b_j}^2)$ on \mathbb{T}^{2N} , reflecting the Abelian nature of the underlying bosonic algebra. The distinct dynamical signatures of each Pauli gate are illustrated in Fig. 1, where Z_j generates straight-line phase translations, while X_j and Y_j produce characteristic oscillatory flows with fixed points at their respective eigenstate phases. Moreover, the Poisson bracket $\{H_A, H_B\} = \omega(X_A, X_B)$ reproduces the $\mathfrak{su}(2)$ Lie algebra: $\{H_X, H_Y\} = H_Z$, etc., confirming that the Pauli gates realize the spin algebra as canonical transformations on phase space.

- **Hadamard as a nonlinear automorphism:** The Hadamard transformation induces a diffeomorphism $\mathcal{H}_j : \mathbb{T}^2 \rightarrow \mathbb{T}^2$ on the 2-torus associated with qubit j :

$$\begin{pmatrix} \phi'_{a_j} \\ \phi'_{b_j} \end{pmatrix} = \begin{pmatrix} \arg(1 + e^{i\Delta\phi_j}) \\ \arg(1 - e^{i\Delta\phi_j}) \end{pmatrix} + \frac{\Sigma\phi_j}{2} \begin{pmatrix} 1 \\ 1 \end{pmatrix},$$

where $\Sigma\phi_j = \phi_{a_j} + \phi_{b_j}$ and $\Delta\phi_j = \phi_{a_j} - \phi_{b_j}$. This map is:

- *Nonlinear*: The output phases depend nontrivially on $\Delta\phi_j$ via trigonometric functions.
- *Singular*: At $\Delta\phi_j = \pi \bmod 2\pi$, the argument becomes undefined (corresponding to the state $|1\rangle$ mapping to $|-\rangle$, which has a phase ambiguity).
- *Area-preserving*: The Jacobian determinant satisfies $\det(D\mathcal{H}_j) = 1$, ensuring unitarity.

Thus, Hadamard implements a nonlinear shear on the torus, mixing the sum and difference coordinates in a phase-dependent way.

- **Multi-qubit gates as entangling diffeomorphisms**: Gates like CNOT and SWAP induce correlations between distinct toroidal factors. For example:

- *SWAP* acts as a permutation of toroidal coordinates: $(\phi_{a_j}, \phi_{b_j}, \phi_{a_k}, \phi_{b_k}) \mapsto (\phi_{a_k}, \phi_{b_k}, \phi_{a_j}, \phi_{b_j})$, which is a global isometry of \mathbb{T}^{2N} .
- *CNOT* implements a conditional flow: the vector field on the target qubit's torus is activated only when the control qubit's phase satisfies $\phi_{b_c} = 0 \bmod 2\pi$ (i.e., the control is in $|0\rangle$). This creates a fiber bundle structure over the control torus, with the target dynamics twisting along the base.

These operations generate the full group of volume-preserving diffeomorphisms on \mathbb{T}^{2N} , enabling universal quantum computation through geometric manipulation of phase space.

This geometric perspective reveals that quantum computation can be viewed as the controlled navigation of a point (or wavefunction) on a high-dimensional torus, where gates correspond to carefully engineered flows and deformations. The topological properties of \mathbb{T}^{2N} —such as its nontrivial fundamental group $\pi_1(\mathbb{T}^{2N}) = \mathbb{Z}^{2N}$ —underlie the robustness of quantum phases and enable topological error correction schemes [13, 16]. Furthermore, the restriction to $|z| = 1$ isolates the essential phase degrees of freedom, providing a minimal yet complete description of qubit dynamics in terms of classical-like phase space trajectories.

This representation is particularly useful for analyzing: Phase coherence properties of quantum states, topological features of quantum circuits, and semiclassical limits where phase dynamics dominate. The unit magnitude constraint $|z| = 1$ effectively projects the full Segal-Bargmann space onto its boundary, capturing the essential phase information while eliminating redundant amplitude degrees of freedom. This provides a minimal representation sufficient for describing all quantum computational processes within the physical subspace.

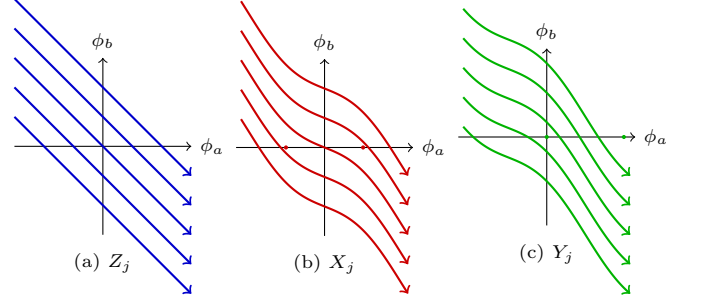


FIG. 1. Phase portraits of Pauli gate dynamics on the (ϕ_{a_j}, ϕ_{b_j}) plane. (a) Z_j : Uniform translation along $\Delta\phi_j = \phi_{a_j} - \phi_{b_j}$ (straight lines of constant $\Sigma\phi_j$). (b) X_j : Nonlinear oscillations with fixed points at $\Delta\phi_j = \pm\pi/2$ (eigenstates $|\pm\rangle$). (c) Y_j : Oscillations with fixed points at $\Delta\phi_j = 0, \pi$ (eigenstates $|\pm_i\rangle$). All flows preserve $\Sigma\phi_j = \phi_{a_j} + \phi_{b_j}$, reflecting the homogeneity constraint.

V. BEYOND THE TORUS: GEOMETRIC STRUCTURES IN HOLOMORPHIC QUANTUM COMPUTATION

While the toroidal restriction $|z_{a_j}| = |z_{b_j}| = 1$ (i.e., $z = e^{i\phi}$) captures the essential phase dynamics of unitary quantum gates, it discards amplitude information critical for non-unitary processes (e.g., decoherence, measurement, dissipation), state preparation, and gradient-based optimization in variational quantum algorithms. The full Segal-Bargmann space \mathcal{H}_{SB} carries a natural Kähler structure that restores this missing information and reveals deeper geometric features of quantum computation.

A. Amplitude Dynamics in Full Kähler Space

The Segal-Bargmann space \mathcal{H}_{SB} is endowed with a Kähler potential

$$K(\mathbf{z}, \bar{\mathbf{z}}) = \|\mathbf{z}\|^2 = \sum_{j=1}^N (|z_{a_j}|^2 + |z_{b_j}|^2), \quad (40)$$

which induces a compatible triple of geometric structures:

- A **Riemannian metric** $g_{i\bar{j}} = \partial_i \partial_{\bar{j}} K = \delta_{ij}$, which defines distances between quantum states via the fidelity $F(\psi, \phi) = |\langle \psi | \phi \rangle|^2$.
- A **symplectic form** $\omega = i \sum_j dz_j \wedge d\bar{z}_j$, which governs Hamiltonian evolution through the equation $\dot{z}_j = -i \partial_{\bar{z}_j} H$.
- A **complex structure** J (multiplication by i), which encodes the uncertainty principle.

In non-unitary scenarios (e.g., Lindblad dynamics), the amplitude degrees of freedom $|z_j|$ evolve according to dissipative flows on \mathbb{C}^{2N} , while the toroidal subspace \mathbb{T}^{2N}

remains invariant only under purely unitary evolution. Thus, simulations of open quantum systems require the full Kähler geometry to capture relaxation toward fixed points (e.g., thermal states).

B. Entanglement Geometry via Segre Embedding

The physical state space for N qubits is the complex projective space $\mathbb{C}P^{2^N-1}$, equipped with the Fubini–Study metric [14, 15]

$$ds_{\text{FS}}^2 = \frac{\langle d\psi | d\psi \rangle}{\langle \psi | \psi \rangle} - \frac{|\langle \psi | d\psi \rangle|^2}{\langle \psi | \psi \rangle^2}, \quad (41)$$

which induces the quantum fidelity distance $D_{\text{FS}}([\psi], [\phi]) = \arccos \sqrt{|\langle \psi | \phi \rangle|^2 / (\langle \psi | \psi \rangle \langle \phi | \phi \rangle)}$. Within this space, separable (unentangled) states form a lower-dimensional submanifold—the Segre variety (product) [17, 18] :

$$\Sigma_N = \underbrace{\mathbb{C}P^1 \times \cdots \times \mathbb{C}P^1}_{N \text{ times}} \hookrightarrow \mathbb{C}P^{2^N-1}. \quad (42)$$

In the holomorphic representation, a state is separable if and only if its Segal–Bargmann function factorizes:

$$f(\mathbf{z}) = \prod_{j=1}^N (c_{0j} z_{a_j} + c_{1j} z_{b_j}). \quad (43)$$

Entangling gates like CNOT act as diffeomorphisms that map Σ_N to its complement:

$$\text{CNOT}_{c,t} : \Sigma_N \rightarrow \mathbb{C}P^{2^N-1} \setminus \Sigma_N. \quad (44)$$

For example, applying CNOT to the separable state $f = z_{a_c} z_{a_t}$ yields:

$$f' = z_{a_c} z_{a_t} + z_{b_c} z_{b_t}, \quad (45)$$

which is non-factorizable and corresponds to the Bell state $|\Phi^+\rangle$. The degree of entanglement can be quantified geometrically by the minimal Fubini–Study distance from the Segre variety:

$$\mathcal{E}([\psi]) = \min_{[\phi] \in \Sigma_N} D_{\text{FS}}([\psi], [\phi]), \quad (46)$$

which vanishes if and only if $[\psi]$ is separable. This provides a powerful visualization tool: entanglement generation is literally the “lifting” of a trajectory off the Segre manifold into the full projective space, with the Fubini–Study metric measuring the geometric cost of entanglement. This geometric perspective is illustrated in Fig. 2, where an entangling gate lifts a quantum state off the Segre submanifold, with the Fubini–Study geodesic measuring the resulting entanglement.

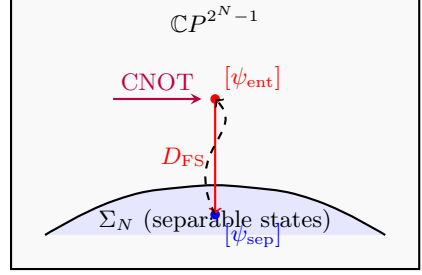


FIG. 2. Schematic illustration of entanglement geometry in projective Hilbert space. The Segre variety Σ_N (blue submanifold) contains all separable states. An entangling gate maps a separable state $[\psi_{\text{sep}}]$ to an entangled state $[\psi_{\text{ent}}]$, with the Fubini–Study distance D_{FS} measuring the minimal geodesic distance to Σ_N . The Fubini–Study distance D_{FS} quantifies the degree of entanglement.

C. Topological Protection from Fiber Bundle Structure

The constraint $|z_{a_j}|^2 + |z_{b_j}|^2 = 1$ for each qubit defines a Hopf fibration [13]:

$$S^1 \hookrightarrow S^3 \xrightarrow{\pi} S^2, \quad (47)$$

where the total space S^3 is the unit sphere in \mathbb{C}^2 (physical states before projectivization), the base space S^2 is the Bloch sphere (physical qubit states), and the fiber S^1 represents the unobservable global phase. For N qubits, this generalizes to a principal $U(1)^N$ -bundle:

$$U(1)^N \hookrightarrow (S^3)^N \xrightarrow{\pi} (S^2)^N. \quad (48)$$

Quantum gates that act locally (e.g., single-qubit rotations) correspond to vertical automorphisms (they move only along fibers), while entangling gates induce horizontal lifts that twist the bundle. Crucially, the holonomy of this bundle—computed via the Berry connection

$$\mathcal{A} = i \sum_j (\bar{z}_{a_j} dz_{a_j} + \bar{z}_{b_j} dz_{b_j}) \quad (49)$$

—is robust against local phase noise. This explains why topological quantum computations are inherently fault-tolerant: errors that act only on the fiber (phase fluctuations) do not affect the base-space computation (the logical qubit state).

D. Semiclassical Limits and Coherent State Path Integrals

The Kähler potential $K = \|\mathbf{z}\|^2$ enables a direct connection to Feynman path integrals via coherent states [19–21]. The transition amplitude between states $|\psi_i\rangle$ and $|\psi_f\rangle$ is given by:

$$\begin{aligned} \langle \psi_f | e^{-iHt} | \psi_i \rangle &= \int \mathcal{D}[\bar{z}, z] \\ &\times \exp \left(i \int_0^t \left[\frac{i}{2} (\bar{z}\dot{z} - \dot{\bar{z}}z) - H(\bar{z}, z) \right] dt' \right), \end{aligned} \quad (50)$$

where the measure $\mathcal{D}[\bar{z}, z]$ is induced by the Kähler metric. In the semiclassical limit ($\hbar \rightarrow 0$), the path integral is dominated by classical trajectories satisfying:

$$i\dot{z}_j = \frac{\partial H}{\partial \bar{z}_j}, \quad (51)$$

$$-i\dot{\bar{z}}_j = \frac{\partial H}{\partial z_j}. \quad (52)$$

These are precisely the Hamiltonian equations on the Kähler manifold. For the gate representations developed in this work:

- Pauli gates correspond to quadratic Hamiltonians, e.g., $H_X = \frac{1}{2}(z_a\bar{z}_b + z_b\bar{z}_a)$,
- The Hadamard gate arises from a time-dependent linear Hamiltonian.

This framework allows semiclassical simulation of quantum circuits by solving Hamiltonian ordinary differential equations (ODEs) on \mathbb{C}^{2N} , with quantum corrections computable via loop expansions in powers of \hbar . Specifically, the path integral

$$\langle \psi_f | e^{-iHt} | \psi_i \rangle = \int \mathcal{D}[\bar{z}, z] \exp \left(\frac{i}{\hbar} S[\bar{z}, z] \right) \quad (53)$$

is evaluated by expanding the action $S[\bar{z}, z] = \int_0^t \left[\frac{i\hbar}{2} (\bar{z}\dot{z} - \dot{\bar{z}}z) - H(\bar{z}, z) \right] dt'$ around its classical stationary point $(\bar{z}_{\text{cl}}, z_{\text{cl}})$ satisfying the Kähler Hamilton equa-

tions. The leading-order contribution yields the semiclassical propagator

$$K_{\text{sc}}(t) = \mathcal{N} \exp \left(\frac{i}{\hbar} S_{\text{cl}} \right), \quad (54)$$

where $S_{\text{cl}} = S[\bar{z}_{\text{cl}}, z_{\text{cl}}]$ and \mathcal{N} is a prefactor determined by Gaussian fluctuations. Higher-order quantum corrections arise from evaluating functional determinants of the fluctuation operator, which correspond to loop diagrams in the associated field theory. For weakly entangled states—those remaining near the Segre variety Σ_N during evolution—these fluctuations are suppressed, making the semiclassical approximation particularly accurate and computationally efficient compared to full Hilbert space simulations.

VI. CONCLUSION

We have established a comprehensive framework for representing quantum logic gates in the Segal–Bargmann space. First, we derived explicit differential operator forms for fundamental single- and multi-qubit gates—including Pauli operators, Hadamard, SWAP, CNOT, and CZ—acting on holomorphic variables z_{a_j}, z_{b_j} . Crucially, we demonstrated that physical qubit states correspond to functions homogeneous of degree one in each bosonic pair, and all quantum gates preserve this constraint while implementing unitary transformations. The restriction to unit-magnitude variables ($|z| = 1$) reveals a toroidal space \mathbb{T}^{2N} where gates act as canonical transformations: Pauli operators generate Hamiltonian flows, Hadamard implements a nonlinear automorphism, and entangling gates create correlations between distinct toroidal factors. Beyond the torus, the full Kähler geometry of the Segal–Bargmann space provides a richer structure that captures amplitude dynamics essential for non-unitary processes, while the Segre embedding offers a geometric characterization of entanglement as deviation from separable manifolds. The underlying fiber bundle structure explains topological protection against phase noise, and the Kähler potential enables semiclassical simulations via coherent state path integrals.

[1] F. Strocchi, *Complex Coordinates and Quantum Mechanics*, Rev. Mod. Phys. **38**, 36 (1966).

[2] W. P. Schleich, *Quantum Optics in Phase Space* (Wiley-VCH, Berlin, 2001).

[3] C. K. Zachos, D. B. Fairlie, T. L. Curtright, *Quantum mechanics in phase space: an overview with selected papers*, World Scientific 2005.

[4] S. L. Braunstein and P. van Loock, *Quantum information with continuous variables*, Rev. Mod. Phys. **77**, 513 (2005).

[5] C. Miquel, J. P. Paz, M. Saraceno, *Quantum computers in phase space*, Phys. Rev. A **65**, 062309 (2002).

[6] I. E. Segal, *Mathematical problems of relativistic physics*, in Kac, M. (ed.), *Proceedings of the Summer Seminar*, Boulder, Colorado, 1960, Vol. II, *Lectures in Applied Mathematics*, American Mathematical Society (1963).

[7] V. Bargmann, *On a Hilbert space of analytic functions and an associated integral transform part I*, Commun. Pure. Appl. Math. **14** (3): 187 (1961).

[8] A. Perelomov, *Generalized Coherent States and Their Applications*, Springer Berlin, Heidelberg (1986).

- [9] G. B. Folland, *Harmonic Analysis in Phase Space*, Princeton University Press (1989).
- [10] A. Vourdas, R. F. Bishop, *Thermal coherent states in the Bargmann representation*, Phys. Rev. A **50**, 3331 (1994).
- [11] B. C. Hall, *Holomorphic methods in analysis and mathematical physics*, n, “First Summer School in Analysis and Mathematical Physics” (S. Pérez-Esteva and C. Villegas-Blas, Eds.), 1-59, Contemp. Math. **260**, Amer. Math. Soc., 2000. 0706:P06013, (2007).
- [12] M. W. AlMasri, and M. R. B. Wahiddin, *Bargmann representation of quantum absorption refrigerators*, Rep. Math. Phys. **89** (2), Pages 185-198 (2022).
- [13] A. Hatcher, *Algebraic Topology*, Cambridge University Press (2002).
- [14] J. P. Provost and G. Vallee, *Riemannian structure on manifolds of quantum states*, Commun. Math. Phys. **76**, 289 (1980).
- [15] I. Bengtsson and K. Życzkowski, *Geometry of Quantum States: An Introduction to Quantum Entanglement*, 2nd edition, Cambridge University Press (2017).
- [16] J. K. Pachos, *Introduction to Topological Quantum Computation* (Cambridge University Press, Cambridge, 2012).
- [17] H. Heydari, *Segre variety, conifold, Hopf fibration, and separable multi-qubit states*, Quantum Information and Computation **6** (2006) 400-409
- [18] F. Holweck, J.-G. Luque, and J.-Y. Thibon, *Geometric descriptions of entangled states*, J. Math. Phys. **53** 102203 (2012)
- [19] J. R. Klauder, *The action option and a Feynman quantization of spinor fields in terms of ordinary c-numbers*, Ann. Phys. (N.Y.) **11**, 123 (1960).
- [20] W. D. Kirwin, *Coherent States in Geometric Quantization*, J. Geom. Phys. **57** (2007), no. 2, pages 531 – 548
- [21] S. T. Ali, J.-P. Antoine, and J.-P. Gazeau, *Coherent States, Wavelets, and Their Generalizations*, 2nd ed., Theoretical and Mathematical Physics (Springer, New York, 2014).